Regulation of Human Melanoma Growth and Metastasis by AGE–AGE Receptor Interactions

Riichiro Abe,* Tadamichi Shimizu,* Hiroshi Sugawara,* Hirokazu Watanabe,* Hideki Nakamura,* Hiroshi Choei,† Nobuyuki Sasaki,† Sho-ichi Yamagishi,‡ Masayoshi Takeuchi, and Hiroshi Shimizu*

*Department of Dermatology, Hokkaido University Graduate School of Medicine, Sapporo, Japan; †Department of Neuropsychiatry, Sapporo Medical University, Sapporo, Japan; ‡Department of Medicine, Kurume University School of Medicine, Kurume, Japan; Department of Biochemistry, Faculty of Pharmaceutical Science, Hokuriku University, Kanazawa, Japan.

Advanced glycation end products (AGE), nonenzymatically glycated protein derivatives, have been implicated in the development and progression of diabetic angiopathies, including skin dermopathy. Nevertheless, the involvement of AGE in the development and progression of melanoma has not been fully elucidated. In this study we investigated the expression levels of their receptor for AGE (RAGE) in human melanoma and subsequently studied the effects of AGE on melanoma growth and migration. First, RAGE was detected in the cytoplasm of human melanoma cells (G361 and A375). Among the different types of AGE, glyceraldehyde- and glycolaldehyde-derived AGE significantly stimulated the growth and migration of human melanoma cells. Furthermore, tumor formation of melanoma cell xenografts in athymic mice was prevented by treatment with anti-RAGE neutralizing antibodies. In tumor-bearing mice, survival rates were prolonged, and spontaneous pulmonary metastases were inhibited by treatment using anti-RAGE neutralizing antibodies. In addition, all AGE were present in beds of human melanoma tumor, whereas they were barely detected in normal skin. These results suggest that AGE might be involved in the growth and invasion of melanoma through interactions with RAGE and represent promising candidates for assessing the future therapeutic potential of this therapy in treating patients with melanoma.

Key words: migration/invasion.
J Invest Dermatol 122:461–467, 2004

The main cause of treatment failure and death for cancer patients is metastasis—the formation of secondary tumors in organs a long way from the original cancer. Among cancers, melanoma is the most highly invasive and metastatic tumor with an incidence and mortality that have been rapidly increasing above those of any other cancers in recent year (Morton *et al*, 1993). Adjuvant therapy of proven efficacy is not currently available for these patients; therefore, the search for new targets for therapeutic reagents is required to prevent both proliferation and metastasis. Nevertheless, the molecular and genetic events that contribute to the formation and progression of cutaneous melanoma are poorly understood. It has been reported that oxidative stress contributes to the pathogenesis of melanoma. Indeed, ultraviolet irradiation, one of the highest risk factors for melanoma (McKie, 1998; Noonan, 2001), causes oxidative DNA damage that is additionally potentially mutagenic (Setlow *et al*, 1993).

Advanced glycation end products (AGE), nonenzymatically glycated protein derivatives, were originally known to accumulate in various tissues and have been implicated in the development of diabetic vascular complications, for example, retinopathy and nephropathy (Yang *et al*, 1994; Stitt *et al*, 1997). Recent studies demonstrated that AGE synthesis is accelerated by intra- and extracellular oxide stress (Mullarkey *et al*, 1990). The receptor for advanced glycation end products (RAGE), a multiligand member of the immunoglobulin superfamily of cell surface molecules, interacts with distinct molecules implicated in homeostasis, development, and inflammation (Schmidt *et al*, 2001). Binding RAGE by a ligand triggers activation of key cell-signaling pathways, thereby reprogramming cellular properties. Recently Taguchi and colleagues (2000) have identified RAGE in a molecular checkpoint that regulates not only the invasiveness but also the growth and movement of glioma cells. Nevertheless, the role of RAGE is still unclear in melanoma proliferation and metastasis. One of the hypotheses for the pathogenesis of melanoma growth and migration suggests that AGE formed at an accelerated rate under oxidative stress conditions might be involved in the growth and invasion of melanoma through the interactions with RAGE. In addition, we have previously elucidated the pathways of AGE formation and characterized distinct AGE classes (AGE1–5) and their different cell-mediated responses (Takeuchi *et al*, 1999, 2000a, b).

The aim of this study was to investigate whether distinct AGE–RAGE interactions are a potential enhancer for growth and/or cell migration in human melanoma cell.

Abbreviations: AGE, advanced glycation end product; CML, *N*-(carboxymethyl)lysine; PBS, phosphate-buffered saline; PBS-T, PBS-Tween; RAGE, receptor for advanced glycation end product.

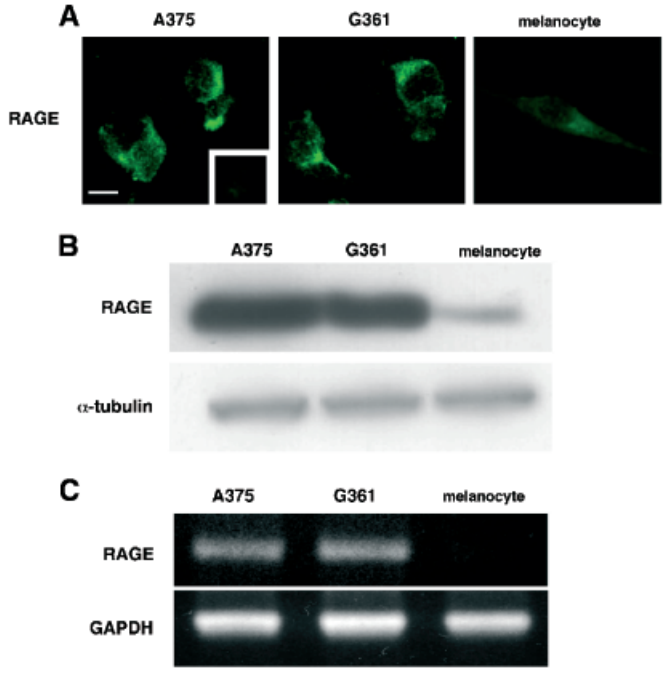

Figure 1
RAGE is expressed in human melanoma cell. (*A*) A375 and G361 melanoma cells cultured on slides were analyzed for RAGE using confocal fluorescence microscopy. Control panels indicate the staining with control IgG. *Bars*, 10 μm. (*B*) RAGE (35 kDa) and α-tubulin (50 kDa) were analyzed by western blot of melanoma cells (A375, G361) and melanocyte lysates. (*C*) RT-PCR was performed with RNA isolated from melanoma cells (A375, G361) and melanocytes and degenerate primers based on the RAGE and glyceraldehyde-3-phosphate dehydrogenase amino acid sequences.

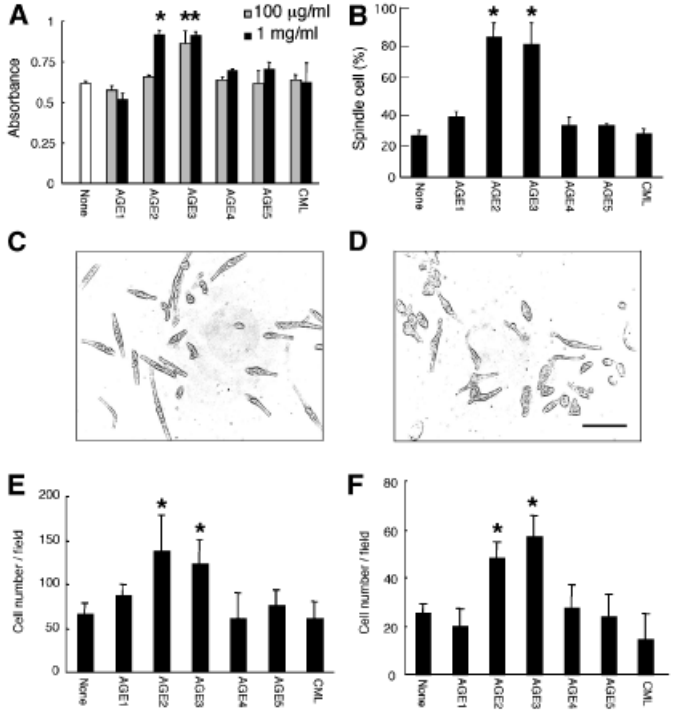

Figure 2
AGE2- and AGE3-induced melanoma cell proliferation, migration, and invasion *in vitro*. The medium of G361 melanoma cells was added each AGE or CML (100 μg/mL or 1 mg/mL) for 48 h. (*A*) Proliferation was assessed by WST-1 assay. *$p<0.01$ compared with medium alone. (*B*) G361 cells were treated with AGE (1 mg/mL) and cultured on plastic dishes coated with purified collagen I. After 18 h of incubation, cells were photographed under phase contrast microscopy. (*C*) AGE2; (*D*) no addition. *Bars*, 50 μm. The spreading cells are counted as spindle cells if they had a length/width ratio greater than three. *$p<0.005$ compared with medium alone. In migration and invasion assay, G361 cells were layered on top of the membrane of Transwell devices (*E*) or Matrigel-coated membrane (*F*). Cells were allowed to migrate through the membrane for 16 h (migration assay) or 48 h (invasion assay). Transmigrated cells were counted by crystal violet staining. *$p<0.005$ compared with medium alone.

Results

RAGE expressed in human melanoma cells To investigate whether RAGE proteins are detected in human melanoma, melanoma cell lines (G361 and A375) and normal melanocyte were immunohistochemically examined using antibodies against RAGE. The results showed the presence of RAGE protein in the membrane and cytoplasm of these melanoma cells (Fig 1*A*), which is similarly staining pattern with astrocytes (Sasaki *et al*, 2001). Melanocyte expressed RAGE weakly compared melanoma cell. This was confirmed by western blotting experiments in which RAGE (35 kDa) was detected in melanoma cell extractions, whereas normal melanocyte extraction contained lower level of RAGE (Fig 1*B*). To further confirm these RAGE expression results, quantitative analyses of RAGE mRNA expression were undertaken using RT-PCR. The results showed that RAGE mRNA (262 bp) was detected in two melanoma cell lines (Fig 1*C*). Nevertheless, it was barely detected in normal melanocytes. These data give a consistent representation of RAGE expression observed in the melanoma cell lines.

AGE2- and AGE3-induced cell proliferation of melanoma cells *in vitro* The next experiment determined which AGE induce melanoma cell growth *in vitro*. The immunochemically distinct AGE (AGE1, glucose-derived AGE; AGE2, glyceraldehyde-derived AGE; AGE3, glycolaldehyde-derived AGE; AGE4, methylglyoxal-derived AGE; AGE5, glyoxal-derived AGE) (Takeuchi *et al*, 1999, 2000a, b) were used. Various concentrations (0–1 mg/mL) of AGE were added to the culture medium of G361 cells. Cell growth was assessed using a modified MTS assay after a 48-h incubation with the added compounds. Significant growth stimulation with the addition of AGE2 and AGE3 was observed ($p<0.01$), whereas other AGE failed to enhance cell proliferation (Fig 2*A*).

AGE2- and AGE3-induced migration and invasion in melanoma cells *in vitro* Previous report indicated that RAGE mediates migration of glioma cells (Taguchi *et al*, 2000); therefore, we then assessed these properties in melanoma cells *in vitro*. First, we observed the morphologic changes by caused the addition of AGE, involved in their ability to extend processes necessary to migrate into the surrounding matrix. The spreading cells were counted as spindle cells if they showed a length-to-width ratio of more than 3 (Fig 2*B–D*). The population of spindle cells was 24% when G361 cells were cultured with no addition on collagen-I-coated matrix. Only AGE2 and AGE3 increased spindle cells population to 81% and 77, respectively

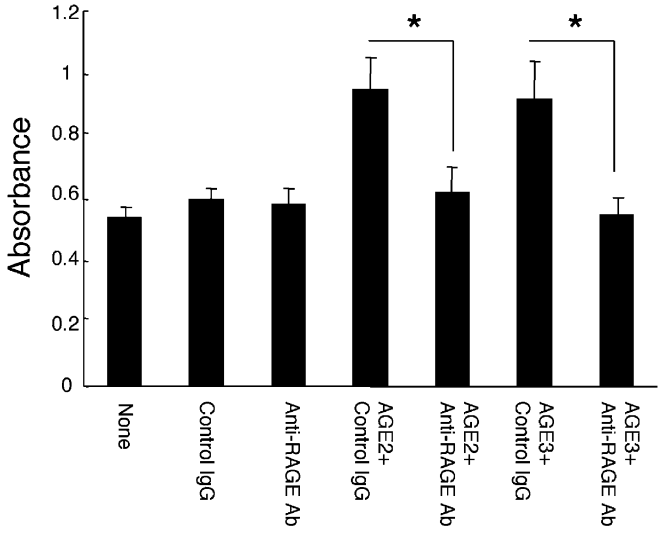

Figure 3
Anti-RAGE antibody inhibited the melanoma cell proliferation induced by AGE2 and AGE3. The medium of G361 was added with each AGE2 and AGE3 (1 mg/mL), anti-RAGE antibody (10 μg/mL), of control IgG (10 μg/mL) as indicated for 48 h at 37°C. The proliferations were assessed by WST-1 assay. *$p < 0.005$.

($p < 0.005$). To explore whether AGE enhance melanoma cell migration and invasion, G361 cells were examined in migration and invasion assays. The migration of G361 cells was significantly enhanced by 138 and 108% by AGE2 and AGE3, respectively ($p < 0.005$) (Fig 2*E*). Similarly, during invasion assays, numbers of invading cells, which were able to degradate Matrigel, also increased with the addition of AGE2 and AGE3 ($p < 0.005$) (Fig 2*F*).

Anti-RAGE antibody inhibited melanoma cell proliferation induced by AGE2 and AGE3 It was investigated whether anti-RAGE antibodies could inhibit AGE-induced melanoma cell proliferation. This antibody was shown to neutralize RAGE engagement; namely, it completely inhibited G361 cell proliferation stimulated by either AGE2 or AGE3 (Fig 3).

RAGE blockade suppressed growth of implanted melanoma in immunocompetent mouse Next we analyzed the effects of anti-RAGE antibodies on the growth of melanoma tumors using G361 melanoma xenografts *in vivo*. Initially, mice were subcutaneously injected with G361 cells into their upper flanks. After 10 d mice were treated intraperitoneally with 0.5 mg of either anti-RAGE antibody or control IgG, once every 5 d. The mouse tumors treated with the control antibody continued their aggressive growth to reach the size of 400 mm^3 by day 30 (Fig 4*A*). In contrast, treatment with anti-RAGE antibody resulted in a significant twofold reduction in tumor size compared with control IgG-treated mice ($n = 5$/group, $p < 0.01$). To determine whether RAGE tumor growth inhibition was associated with inhibition of tumor blood vessel formation, tumor fragments were processed for histologic examination. Because the number of capillaries was not different between tumor-treated anti-RAGE antibodies and control IgG (Fig 4*B,C*), this tumor

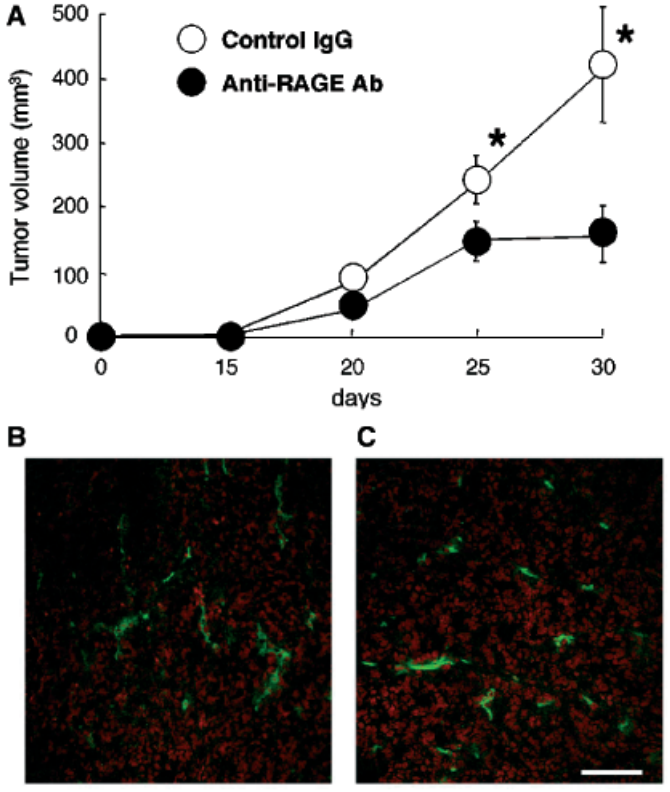

Figure 4
RAGE blockade suppressed growth of implanted G361 melanoma, not by inhibition of angiogenesis. (*A*) G361 melanoma cells (5×10^6) were injected subcutaneously into the upper flank of Balb/c-nu/nu mice ($n = 5$/group). Mice received intraperitoneal injections of PBS, control IgG (0.5 mg), or anti-RAGE antibodies (0.5 mg) after 10 d; they were injected every 5 days. Tumor weights (average ± SD) were measured. *$p < 0.01$. For immunohistochemical analysis of microvessels in the tumor tissues, sections were stained with anti-CD34 (*FITC, green*) antibody. Nuclei were stained with propidium iodide (*red*). Microvessels in the anti-RAGE antibody-treated melanoma tissues (*B*) and control IgG-treated melanoma tissue (*C*). *Bars*, 50 μm.

growth suppression was not induced by inhibition of angiogenesis.

RAGE blockade prolonged survival of tumor-bearing mice and inhibited spontaneous lung metastasis G361 cells (1×10^6) were injected intraperitoneally into nude mice to evaluate the effect of anti-RAGE antibody on the mortality rate. Mice received intraperitoneal injections of 0.3 mL of either control IgG (0.5 mg) or anti-RAGE antibody (0.5 mg) 10 d later and once every 5 d. The survival time of tumor-bearing mice injected with anti-RAGE antibody was significantly longer than tumor-bearing mice injected with control IgG ($n = 5$/group, $p < 0.05$) (Fig 5*A*).

Next, we examined whether anti-RAGE antibodies influenced metastasis *in vivo*. When the tumor volume size established by the initial G361 injection into the upper flank of nude mice reached 500 mm^3, primary tumors were excised. Mice were then maintained for an additional 3 wk to allow further growth of lung metastases. Mice received intraperitoneal injections of 0.3 mL of control IgG (0.5 mg) or anti-RAGE antibody (0.5 mg) once every 3 d after tumors were removed. The number of macroscopic surface lung colonies per mouse was used as a parameter for judging

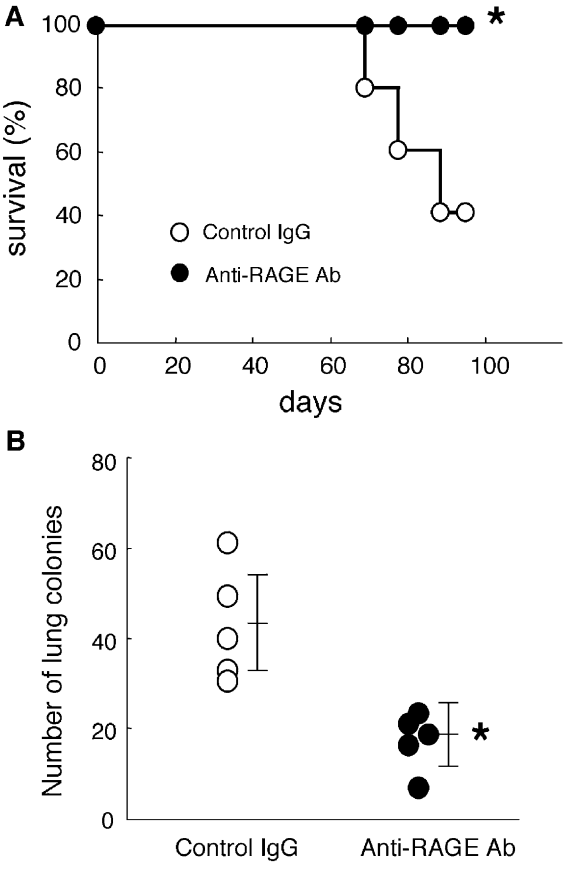

Figure 5
RAGE blockade prolonged survival of tumor-bearing mouse and inhibited spontaneous lung metastasis. (*A*) A single-cell suspension of 1×10^6 G361 melanoma cells was injected into the peritoneal cavity of 6-wk-old female athymic nude mice (n = 5/group). Mice received intraperitoneal injections of 0.3 mL of control IgG (0.5 mg) or anti-RAGE antibodies (0.5 mg) after 10 d and once per 5 days. Mice were then observed for survival, which was recorded as the percentage of surviving animals over time (in days) after tumor injection. $^*p < 0.01$. (*B*) 1×10^6 G361 cells were injected into the upper flank of nude mice (n = 5/group). When the mean tumor volume reached 500 mm^3, primary tumors were removed. Mice were then maintained for an additional 3 wk to allow further growth of lung metastases. Mice received intraperitoneal injections of control IgG (0.5 mg) or anti-RAGE antibodies (0.5 mg) once every 3 d after tumors were removed. The mice were necropsied, and the lungs were removed. Visible lung metastases were counted with the aid of a dissecting microscope. $^*p < 0.01$.

the lung colonization efficiency. The metastatic efficiency was markedly reduced in mice treated with anti-RAGE antibody (n = 5/group, $p < 0.05$) (Fig 5*B*).

AGE and RAGE expressed in human melanoma tissue To investigate whether AGE and RAGE proteins are detected in human melanoma *in vivo*, human melanoma specimens were immunohistochemically examined for antibodies against various types of immunochemically distinct AGE (AGE1-5), CML, and RAGE. The results showed that AGE2 was strongly present within cytoplasm of melanoma cells and in the extracellular matrix (Fig 6*A*). All of other AGE and CML were similarly stained (data not shown). In contrast, RAGE was detected only in cytoplasm of melanoma cells. In normal skin, AGE and CML were hardly detected, and also RAGE was hardly stained in melanocytes (data not shown).

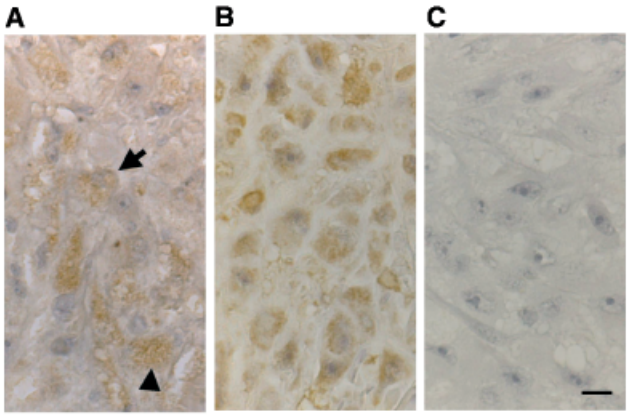

Figure 6
AGE and RAGE are expressed in human melanoma. Immunohistochemical preparations stained with anti-AGE2 (*A*), anti-RAGE (*B*), and control IgG (*C*) using the avidin-biotin immunoperoxidase method. The data of other AGE and CML were not shown. (*A, arrow*) Intracellular and (*arrowhead*) extracellular AGE2 localization. *Bars*, 10 μm.

Discussion

Here we demonstrate that RAGE was expressed in human melanoma cells. Furthermore, glyceraldehyde-derived AGE (AGE2) and glycolaldehyde-derived AGE (AGE3) enhanced proliferation, migration, and invasion of this melanoma cell line *in vitro*. Finally, the treatment by intraperitoneal injection of the neutralizing anti-RAGE antibody reduced local tumor formation, prolonged survival rate, and inhibited lung metastases in nude mice.

It has been reported that RAGE is expressed by a range of cell types, including endothelial cell, astrocytes, and some malignant cells such as malignant glioma and squamous cell carcinoma, contributing to homeostasis, development, inflammation, and carcinogenesis (Mullarkey *et al*, 1990; Yamagishi *et al*, 1997; Yamamoto *et al*, 1995; Sasaki *et al*, 1998). We and other groups have reported that AGE were present in various tissues including endothelial cells of blood vessel, mesenchymal cells, and extracellular matrix (Ling *et al*, 1998; Mizutari *et al*, 1997). Accumulation of AGE initiated various important processes including angiogenesis in diabetic microangiopathies (Yamagishi *et al*, 1997). AGE formation in the extracellular matrix of skin is accelerated by ultraviolet-induced oxidation (Mizutari *et al*, 1997), and AGE generate active oxygen species in the skin during ultraviolet irradiation (Masaki *et al*, 1997), suggesting the presence of vicious cycle of AGE formation. Furthermore, AGE can activate RAGE expression causing enhanced AGE–RAGE interaction (Tanaka *et al*, 2000). It is thus hypothesized that activated cells that include not only tumor cells but also stromal cells located in peritumor site synthesize AGE. Taken together, we hypothesize that convenient for melanoma cells proliferate and invade with abundant accumulation of extracellular AGE in skin.

We have highlighted the pathways of AGE formation and characterized distinct AGE classes (AGE1–5) with different cell-mediated responses (Takeuchi *et al*, 1999, 2000a, b). In this study, AGE2 and AGE3 but not other AGE, can upregulate melanoma cell growth, migration, and invasion *in vitro*. Recently, we also reported strong RAGE binding by

AGE2 and AGE3, but not other AGE (Yonekura *et al*, 2003). Taken together, AGE2– and AGE3–RAGE interactions have an important role in the progression of melanoma. Although previous papers reported that CML–RAGE interaction mediates cell signaling (Kislinger *et al*, 1999), our data showed CML influence little effects on melanoma proliferation, migration, and invasion. We speculate that this disparity is dependent on cell types or transformation (malignant or normal).

We also assessed the therapeutic efficacy of AGE–RAGE interactions in a xenograft model. In our experiments, blocking RAGE by the systemic administration of neutralizing RAGE antibody significantly inhibited the growth of G361 xenograft tumors and spontaneous lung metastasis. Furthermore, the blockade of RAGE prolonged the survival of G361 tumor-bearing mice. Previously we reported that this interaction could play a significant role in the progression of pancreatic cancer through the induction of autocrine platelet-derived growth factor-B (Yamamoto *et al*, 1995). Furthermore, Taguchi and associates (2000) showed that this interaction regulates not only the growth but also the movement and invasiveness of glioma tumor cells (Mullarkey *et al*, 1990). In addition, the presence of AGE was confirmed in human melanoma beds, whereas those were barely detected in normal skin, indicating that the interaction of upregulated RAGE in melanoma cells and AGE that are present in tumor beds promotes melanoma progression. We concluded that these interactions regulate various malignant tumors, which have a particularly high invasive and metastatic potential.

In conclusion, our findings have identified a pivotal role for AGE–RAGE interactions in human melanoma growth and metastasis. We suggested that blockage of these interactions, including using the anti-RAGE antibody are represent a good candidates for treatment of patients with melanoma.

Materials and Methods

Human melanoma specimens Two consecutive cases of melanoma tissue biopsies taken for routine diagnosis with patient consent and ethical permission were retrieved from the Department of Dermatology, Hokkaido University Graduate School of Medicine.

Mice and cell lines Balb/c-nu/nu mice were purchased from Japan Clea (Tokyo, Japan) and maintained under specific pathogen-free conditions. All animal procedures were conducted according to guidelines from the Hokkaido University Institutional Animal Care and Use Committee under an approved protocol. The two human melanoma cell lines, G361 and A375 (American Type Culture Collection, Manassas, VA) were maintained in RPMI 1640 supplemented with 10% fetal calf serum, 100 units per mL penicillin/streptomycin. Normal human neonatal melanocytes were purchased from Kurabo (Osaka, Japan) and were cultured according to the manufacturer's instructions.

Preparation of AGE proteins and *N*-(carboxymethyl)lysine–bovine serum albumin AGE–bovine serum albumin and AGE–rabbit serum albumin were prepared as described previously (AGE1, glucose-derived AGE; AGE2, glyceraldehyde-derived AGE; AGE3, glycolaldehyde-derived AGE; AGE4, methylglyoxal-derived AGE; AGE5, glyoxal-derived AGE) (Takeuchi *et al*, 1999, 2000a, b). Carboxymethyllysine (CML)–bovine serum albumin was prepared as described elsewhere (Ikeda *et al*, 1996). Protein concentrations were determined with the DC protein assay reagent (Bio-Rad Laboratories, Richmond, CA) using bovine serum albumin as a standard.

Preparation of antibodies A polyclonal antibody against RAGE was raised in rabbits (Sasaki *et al*, 2001). The peptides were synthesized according to the amino acid sequences of RAGE, residues 167 to 180 in extracellular domain. Synthesized peptide was coupled to keyhole limpet hemocyanin and mixed with an equal volume of Freund's complete adjuvant. The conjugated peptide were injected into rabbits three times at 2-wk intervals. Serum was obtained 2 wk after last injection, and antibody titer was assessed by ELISA. This anti-RAGE antibody certainly recognizes full-length RAGE (Sasaki *et al*, 2001). For *in vivo* experiments, the IgG fraction of antiserum was purified by Sepharose A. Antibodies specific for all AGE (AGE1–5 and CML) were prepared as previously described (Takeuchi *et al*, 1999, 2000a, b).

Immunofluorescence microscopy Immunofluorescence staining was performed on melanoma cells grown on glass coverslips. The glass coverslips were incubated with anti-RAGE antibody (1:100 dilution) overnight at 4°C in Tris-buffered saline containing 1% bovine serum albumin. The primary antibodies were detected using fluorescein isothiocyanate-labeled goat anti-rabbit IgG (Vector Laboratories, Burlingame, CA). The glass coverslips were examined using a confocal laser microscope (laser scanning confocal imaging system Model MRC 1024, Bio-Rad) equipped with an inverted fluorescence microscope (Zeiss, Germany).

Western blot G361, A375, and normal melanocytes were grown to confluence in 100-mm dishes, washed with phosphate-buffered saline (PBS), and lyzed as previously described (Shimizu *et al*, 1999). Samples containing 50 μg of protein were loaded onto 10% acrylamide gels. Proteins were separated by sodium dodecyl sulfate-polyacrylamide gel electrophoresis and electrophoretically transferred to nitrocellulose filters. After transfer, the filters were blocked by incubation with 5% nonfat dry milk in PBS-Tween (PBS-T) buffer overnight at room temperature. The filters were then incubated for 1 h with PBS-T containing 0.1% nonfat dry milk and the anti-RAGE antibody at 1:2500 dilution or α-tubulin antibody (Santa Cruz Biotechnology, Santa Cruz, CA) at 1:1000. Next, the filters were washed three times in PBS-T and incubated with PBS-T containing 0.1% nonfat dry milk and horseradish peroxidase-linked anti-rabbit Ig [$F(ab')_2$] (Amersham-Life Science, Buckinghamshire, UK) diluted 1:5000 for 1 h at room temperature. Filters were washed three more times in PBS-T, and immunoreactivity was detected using an enhanced chemiluminescence western blot detection system (Amersham), followed by exposure to ECL HYPER film (Amersham).

Reverse transcription-polymerase chain reaction In brief, PCR was carried out as previously described (Tanji *et al*, 2000). The sense primer for RAGE was from bp 1801 to bp 1820 (5′-GCCCTCCAGTACTACTCTCG-3′), and the antisense primer was from bp 2043 to bp 2062 (5′-TGTGTGGCCACCCATTCCAG-3′). The sense and antisense primers for glyceraldehyde-3-phosphate dehydrogenase (GAPDH) were from bp 204 to bp 226 (5′-CAATGGAAATCCCATCACCATCT-3′) and from bp 908 to bp 930 (5′-AATGAGCTTGACAAAGTGGTCGT-3′), respectively. The entire RT reaction product was used for PCR amplification. Forty cycles of amplification were performed using a thermal programmer (Perkin Elmer, Wellesley, MA), as follows: denaturation at 94°C for 15 s and annealing and extension at 60°C for 30 s. The PCR products were then electrophoresed on a 1.5% agarose gel stained with ethidium bromide.

Proliferation assay The cell proliferations were assessed by using a modified MTT assay, the WST-1 assay, which is a colorimetric assay based on the cleavage of the tetrazolium salt

WST-1 to a formazan dye by the mitochondrial dehydrogenase of viable cells. G361cells (5×10^3 cells per well) were preincubated for 24 h with serum-free medium at 37°C. The medium was replaced with medium containing each AGE, CML (0–1 mg/mL) or anti-RAGE antibody (10 μg/mL) and control IgG (10 μg/mL) for 48 h at 37°C. The ready-to-use WST-1 reagent (Dojin, Kumamoto, Japan) was added to the cells during the last 4 h and incubated at 37°C. Viable cells were then determined using a microplate reader at 450 nm with a 630-nm reference wavelength.

Transmigration and invasion assays To examine the properties of the tumors grown by AGE, G361 cells were added to plastic dishes (Nunc, Naperville, IL) coated with purified collagen I. After 18 h, cells were photographed under phase contrast microscopy. The spreading cells were counted as spindle cells if they had a length/width ratio greater than 3. In a transmigration assay, the upper side of a modified Boyden chamber polycarbonate membrane (Transwell 24, 8-μm pore, Costar, Cambridge, MA) (Albini *et al*, 1987) either was left uncoated (transmigration) or was coated (invasion) with Matrigel (1 mg/mL) (Matrigel-GFR, Falcon-Becton Dickinson, Bedford, MA) for 2 h at room temperature (Kleinman *et al*, 1986). Cells were then seeded in the upper chambers in their respective culture medium without fetal bovine serum but containing AGE, and incubated for either 16 h (transmigration) or 48 h (invasion) at 37°C. The chambers were fixed and stained with crystal violet. The cells on the lower surface of the filter were counted (two fields/well) using a microscope with a × 10 objective. Each condition was assayed in triplicate, and each experiment was repeated at least three times.

Tumor growth *in vivo* Experiments to determine the effect of anti-RAGE antibodies on G361 tumor growth were performed in Balb/c-nu/nu mice. Cultured G361 cells were washed and resuspended in PBS; subsequently 5×10^6 cells (suspended in 0.1 mL of PBS) were injected subcutaneously into the upper flank of 6-wk-old female athymic nude mice ($n = 5$/group). Mice received intraperitoneal injections of 0.3 mL of control IgG (0.5 mg) or anti-RAGE antibodies (0.5 mg) 10 d later and from then on once every 5 days. Tumor size was estimated on day 30 using orthogonal linear measurements made with Vernier calipers according to the formula volume $(mm^3) = [(\text{width, mm})^2 \times (\text{length, mm})]/2$. This experiment was repeated twice with similar results. Blood vessels in the tumor were visualized by CD34 staining, which was performed on cryosections using the fluorescein isothiocyanate-conjugated rat anti-mouse CD34 (PharMingen, San Diego, CA). Nuclei were stained with propidium iodide.

Survival and in vivo metastasis assays A single-cell suspension of 1×10^6 G361 cells was injected into the peritoneal cavity of 6-wk-old female athymic nude mice ($n = 5$/group). Mice received intraperitoneal injections of 0.3 mL of control IgG (0.5 mg) or anti-RAGE antibodies (0.5 mg) 10 d later and from then every 5 d. Mice were then observed for survival, which was recorded as the percentage of surviving animals over time (in days) after tumor injection. To measure the spontaneous metastasis, 1×10^6 cells were injected into the upper flank of 6-wk-old athymic nude mice ($n = 5$/group). When the mean tumor volume reached 500 mm^3, primary tumors were removed. Mice were then maintained for an additional 3 wk to allow further growth and development of lung metastases. Mice received intraperitoneal injections of 0.3 mL of control IgG (0.5 mg) or anti-RAGE antibodies (0.5 mg) once every 3 d after tumors were removed. The mice were necropsied, and the lungs were removed. Visible lung metastases were counted with the aid of a dissecting microscope.

Immunohistochemical staining Serial paraffin sections were immunostained according to the standard streptavidin-biotin peroxidase technique using a Vectastain ABC elite kit (Vector Laboratories). After incubation with 10% goat serum to eliminate nonspecific binding, these sections were followed by incubation overnight at 4°C with the primary antibodies diluted 1:500 to 1:1000 in PBS. The sections were then sequentially incubated with the biotinylated secondary antibody. Then the sections were counterstained with hematoxylin.

Statistical analysis The data were statistically analyzed for significance by Student's t test, except for the *in vivo* survival assays, which were analyzed using Wilcoxon analysis.

We thank Ms Ayumi Honda for excellent technical assistance and Dr James R. McMillan for his manuscript proofreading.

DOI: 10.1046/j.0022-202X.2004.22218.x

Manuscript received April 10, 2003; revised August 29, 2003; accepted for publication September 9, 2003

Address correspondence to: Riichiro Abe, MD, PhD, Department of Dermatology, Hokkaido University Graduate School of Medicine, N 15 W 7, Kita-ku, Sapporo 060-8638, Japan. Email: aberi@med.hokudai.ac.jp

References

Albini A, Iwamoto Y, Kleinman HK, Martin GR, Aaronson SA, Kozlowski JM, McEwan RN: A rapid *in vitro* assay for quantitating the invasive potential of tumor cells. Cancer Res 47:3239–3245, 1987

Ikeda K, Higashi T, Sano H, *et al*: N (epsilon)-(carboxymethyl) lysine protein adduct is a major immunological epitope in proteins modified with advanced glycation end products of the Maillard reaction. Biochemistry 35:8075–8083, 1996

Kislinger T, Fu C, Huber B, *et al*: (epsilon)-(carboxymethyl) lysine adducts of proteins are ligands for receptor for advanced glycation end products that activate cell signaling pathways and modulate gene expression. J Biol Chem 274:31740–31749, 1999

Kleinman HK, McGarvey ML, Hassell JR, Star VL, Cannon FB, Laurie GW, Martin GR: Basement membrane complexes with biological activity. Biochemistry 25:312–318, 1986

Ling X, Sakashita N, Takeya M, Nagai R, Horiuchi S, Takahashi K: Immunohistochemical distribution and subcellular localization of three distinct specific molecular structures of advanced glycation end products in human tissues. Lab Invest 78:1591–1606, 1998

Masaki H, Okano Y, Sakurai H: Generation of active oxygen species from advanced glycation end-products (AGE) under ultraviolet light A (UVA) irradiation. Biochem Biophys Res Commun 235:306–310, 1997

McKie RM: Incidence, risk factors and prevention of melanoma. Eur J Cancer 34:S3–S6, 1998

Mizutari K, Ono T, Ikeda K, Kayashima K, Horiuchi S: Photo-enhanced modification of human skin elastin in actinic elastosis by N (epsilon)-(carboxymethyl) lysine, one of the glycoxidation products of the Maillard reaction. J Invest Dermatol 108:797–802, 1997

Morton DL, Wong JH, Kikwood JM, Parker RG: Cancer medicine. In: Holland JF, Frei E, Bast RC (eds). Malignant Melanoma, 3rd ed. Philadelphia: Lea & Febiger, 1993; p 1793–1824

Mullarkey CJ, Edelstein D, Brownlee M: Free radical generation by early glycation products: A mechanism for accelerated atherogenesis in diabetes. Biochem Biophys Res Commun 173:932–939, 1990

Noonan FP: Neonatal sunburn and melanoma in mice. Nature 413:271–272, 2001

Sasaki N, Fukatsu R, Tsuzuki K, *et al*: Advanced glycation end products in Alzheimer's disease and other neurodegenerative diseases. Am J Pathol 153:1149–1155, 1998

Sasaki N, Toki S, Chowei H, *et al*: Immunohistochemical distribution of the receptor for advanced glycation end products in neurons and astrocytes in Alzheimer's disease. Brain Res 888:256–262, 2001

Schmidt AM, Yan SD, Yan SF, Stern DM: The multiligand receptor RAGE as a progression factor amplifying immune and inflammatory responses. J Clin Invest 108:949–955, 2001

Setlow R, Grist E, Thompson K, Woodhead AD: Wavelengths effective in induction of malignant melanoma. Proc Natl Acad Sci USA 90:6666–6670, 1993

Shimizu T, Abe R, Nakamura H, Ohkawara A, Suzuki M, Nishihira J: High expression of macrophage migration inhibitory factor in human melanoma cells and its role in tumor cell growth and angiogenesis. Biochem Biophys Res Commun 264:751–758, 1999

Stitt AW, Li YM, Gardiner TA, Bucala R, Archer DB, Vlassara H: Advanced glycation end products (AGE) co-localize with AGE receptors in the retinal vasculature of diabetic and of AGE-infused rats. Am J Pathol 150:523–531, 1997

Taguchi A, Blood DC, del Toro G, *et al*: Blockade of RAGE-amphoterin signaling suppresses tumour growth and metastases. Nature 405:354–360, 2000

Takeuchi M, Bucala R, Suzuki T, *et al*: Neurotoxicity of advanced glycation end-products for cultured cortical neurons. J Neuropathol Exp Neurol 59:1094–1105, 2000a

Takeuchi M, Makita Z, Bucala R, Suzuki T, Koike T, Kameda Y: Immunological evidence that non-carboxymethyllysine advanced glycation end-products are produced from short chain sugars and dicarbonyl compounds *in vivo*. Mol Med 6:114–125, 2000b

Takeuchi M, Makita Z, Yanagisawa K, Kameda Y, Koike T: Detection of noncarboxymethyllysine and carboxymethyllysine advanced glycation end products (AGE) in serum of diabetic patients. Mol Med 5:393–405, 1999

Tanaka N, Yonekura H, Yamagishi S, Fujimori H, Yamamoto Y, Yamamoto H: The receptor for advanced glycation end products is induced by the glycation products themselves and tumor necrosis factor-alpha through nuclear factor-kappa B, and by 17beta-estradiol through Sp-1 in human vascular endothelial cells. J Biol Chem 275:25781–25790, 2000

Tanji N, Markowitz GS, Fu C, *et al*: Expression of advanced glycation end products and their cellular receptor RAGE in diabetic nephropathy and nondiabetic renal disease. J Am Soc Nephrol 11:1656–1666, 2000

Yamagishi S, Yonekura H, Yamamoto Y, *et al*: Advanced glycation end products-driven angiogenesis *in vitro*: Induction of the growth and tube formation of human microvascular endothelial cells through autocrine vascular endothelial growth factor. J Biol Chem 272:8723–8730, 1997

Yamamoto Y, Yamagishi S, Hsu CC, Yamamoto H: Advanced glycation endproducts–receptor interactions stimulate the growth of human pancreatic cancer cells through the induction of platelet-derived growth factor-B. Biochem Biophys Res Commun 213:681–687, 1995

Yang CW, Vlassara H, Peten EP, He CJ, Striker GE, Striker LJ: Advanced glycation end products up-regulate gene expression found in diabetic glomerular disease. Proc Natl Acad Sci USA 91:9436–9440, 1994

Yonekura H, Yamamoto Y, Sakurai S, *et al*: RAGE engagement and vascular cell derangement by short chain-derived advanced glycation endproducts. In: Horiuchi S (ed). International Congress Series 1245. Amsterdam: Elsevier Science, 2002; p 129–135